Al-Turath Journal for Biology (ATJB)
Open Access Journal
Open Access Journal
ISSN Print: 3080-1265
Online : 3080-1273

Original Paper

Effects of Al-Doura Thermal Power Plant Emissions on Soil Quality: A Multivariate Assessment with Long-Term Environmental Projections

Isaac Khalil Ibrahim[1], Asmaa Younis Sabbar[2], Reyam Naji Ajmi[3]

[1]College of Pharmacy, Mustansiriyah University, Baghdad, Iraq
[2]Mustansiriyah University, Baghdad, Iraq
[3]Department of Biological Science, Mustansiriyah University, Baghdad, Iraq

Correspondence email | **isaackhalil@uomustansiriyah.edu.iq**
Received: 28/04/2026 | **Accepted**: 22/06/2026 | **Available online:** 30/06/2026 | **DOI:** https://doi.org/10.63964/atjb.2026.2.6

ABSTRACT
This study determined the effects of industrial pollution from the Al-Doura Thermal Power Station, south of Baghdad, Iraq, on the physicochemical properties and contamination gradient of adjacent soils. A distance-based sampling design was used across three sites: Site A (high pollution, <100 m), Site B (moderate pollution, 300–500 m) and Site C (control, >800 m). Thirty soil samples at two depths (0–10 cm, 10–30 cm) were analysed for pH, electrical conductivity (EC), salinity, organic matter, total petroleum hydrocarbons (TPH), heavy metals (Ni, Pb, Cd, Zn) and soil temperature. All parameters differed significantly among sites, Site A showing the highest values with a progressive decline with distance. One-way ANOVA confirmed significant between-site differences ($p < 0.05$) and Tukey's post-hoc test separated Site A from Sites B and C. Pearson correlation, computed on the full sample-level dataset, showed strong associations between TPH and EC ($r = 0.87$, $p < 0.01$) and between soil temperature and Ni ($r = 0.75$, $p < 0.05$). Principal component analysis (PCA) resolved a primary axis (PC1, 52.8% of variance) dominated by TPH, EC and soil temperature, and a secondary axis (PC2, 23.4%) dominated by heavy metals. A separate, controlled biochar-amendment experiment on heavily contaminated soil markedly reduced TPH, EC and Ni while restoring soil-enzyme activity and crop performance. A conceptual, scenario-based projection suggested accelerated soil degradation and contaminant mobility by 2050, broadly consistent with global estimates of 15–17% cropland degradation. The findings provide a multivariate framework for understanding soil degradation under combined industrial and climatic pressure in semi-arid environments.

KEYWORDS: *soil contamination; thermal-power emissions; total petroleum hydrocarbons; heavy metals; principal component analysis; biochar remediation; soil-quality assessment*

1. INTRODUCTION

Soils are among the most important components of terrestrial ecosystems. They store roughly 80% of the planet's terrestrial organic carbon, cover much of the land surface, and are vital for agricultural production, nutrient cycling and ecosystem functioning [1]. Increasing anthropogenic pressures, especially from industry, are causing severe environmental degradation, reducing soil fertility and microbial activity and introducing organic and metallic pollutants [2]. Petroleum pollution is among the most damaging pressures on soils in industrial settings. Crude oil contains toxic organic constituents—polycyclic aromatic hydrocarbons, heavy long-chain hydrocarbons and metals such as nickel and vanadium—that are chemically stable and environmentally persistent and that alter soil fertility, microbial activity and physicochemical properties such as electrical conductivity, salinity and pH [3]. High concentrations of total petroleum hydrocarbons (TPH) raise organic-matter loading and salinity while lowering water retention, making soils more susceptible to climatic stress [4]. In parallel, global warming intensifies soil pressure: elevated CO_2 and methane raise surface temperatures, alter the hydrological cycle, and accelerate organic-matter decomposition and carbon release [5]. Higher temperatures increase pollutant mobility, the volatility of light hydrocarbons and the solubility of heavy metals, thereby increasing soil toxicity and degradation [6]. Although oil contamination and warming are usually studied separately, their joint influence is important, especially in arid and semi-arid ecosystems [7].

In Iraq, the industrial zones of Baghdad particularly those surrounding the Al-Doura thermal power station—exemplify two co-occurring stressors: oil pollution from crude-oil-fuelled generation and persistent thermal emissions, within a semi-arid environment that is highly responsive to thermal and drought stress. Although industrial impacts on air and water pollution have been studied, no systematic, quantitative investigation has characterised the co-occurring oil-pollution and thermal stressors acting on soils in this area. The present study therefore aims to characterize and quantify the spatial gradients of hydrocarbon, thermal and metal contamination around the station and to assess, using a multivariate framework, the degree to which these stressors co-vary. Because the observational distance-gradient design does not permit a formal factorial pollution × warming interaction test, the working hypothesis that hydrocarbon and thermal stressors act in a coupled rather than independent manner is evaluated through their joint loading and covariance structure correlation and PCA

2. MATERIALS AND METHODS

2.1. Study area

The study was conducted around the Al-Doura Thermal Power Plant in southern Baghdad, Iraq (plant centroid 33.2520° N, 44.3461° E), one of the oldest and largest thermal plants in Iraq, running mostly on crude oil and natural gas, because of its long-term operation and emissions, it is an important contributor of gases, particulates, heavy metals, hydrocarbons, and waste heat. Its proximity to the Tigris River means that there is increased likelihood of contaminants getting into the environment via surface runoff and groundwater flows. The semiarid nature of the environment and hot summer temperatures (above 45°C) means that evaporation is enhanced. Sampling sites were set up in the downwind direction at the following approximate coordinates: Site A (33.2516°N, 44.3469°E; less than 100 meters from the plant border), Site B (33.2498°N, 44.3501°E; 300-500 meters), and the reference site (Site C): (33.2452°N, 44).

2.2. Sampling design

A distance-based design captured the contamination gradient with distance from the station, with zones defined in Table 1. At each zone, five points were sampled independently at two depths (0–10 cm and 10–30 cm), giving 30 soil samples in total. Points were selected by a systematic-random scheme to minimise bias and ensure representative coverage, consistent with established environmental soil-survey procedures [8]. All inferential statistics reported below were performed on these 30 individual samples (sample-level data), not on site means.

Table 1. Sampling scheme and expected contamination levels.

Site code	Distance from plant	Expected contamination	Purpose of sampling
A	< 100 m	High	Direct impact of emissions, oil spills and thermal influence
B	300–500 m	Moderate	Dispersed contamination and atmospheric deposition
C	> 800 m	Low / control	Baseline (reference) soil conditions

2.3. Soil sample collection and handling

Field sampling followed a strict protocol to avoid cross-contamination [8]. Stainless-steel instruments were used to prevent metal leaching in the presence of high hydrocarbon levels. Samples were immediately sealed in sterile airtight containers and labelled with site, depth, GPS coordinates, collection date and field observations. In the laboratory, samples were air-dried under clean conditions and sieved (2 mm) to remove coarse fragments and stones.

2.4. Physicochemical analysis and quality control

Representative samples were analysed for physical and chemical properties using internationally accepted methods. Physical characteristics [9,10]: water content (%) by oven-drying at 105 °C, and texture by sieving and hydrometer particle-size analysis. Chemical characteristics [11,12]: pH and electrical conductivity (EC) in soil:water suspensions using a multi-parameter meter; organic matter by Walkley–Black oxidation or loss-on-ignition; total petroleum hydrocarbons (TPH) by gas chromatography with flame-ionisation detection (GC-FID); and heavy metals (Ni, Pb, Cd, Zn) by flame atomic absorption spectrometry (FAAS).

Heavy metal analysis was done using only FAAS (ICP-MS was not used), while the same machine was used throughout to provide consistent results. The quality control included calibration using certified multi-element standard solution (calibration $R^2 \geq 0.999$), blanking reagents and analytical duplicates, and confirmation using certified reference soil. The method detection limit (mg/kg) was 0.5 (Ni), 1.0 (Pb), 0.05 (Cd) and 0.2 (Zn) for FAAS and 5 (TPH) for GC-FID, while spike recovery was between 90% and 105%. TPH analysis used C10-C40 calibration solution with surrogate recovery check.

Table 2. Soil parameters, analytical techniques and objectives.

Parameter	Analytical method	Purpose
pH	Multi-parameter meter	Contaminant influence on soil acidity
Electrical conductivity (EC)	EC meter	Soluble-salt / contamination load
Organic matter	Walkley–Black / LOI	Fertility and adsorption potential
TPH	GC-FID	Petroleum-hydrocarbon contamination
Heavy metals (Ni, Pb, Cd, Zn)	FAAS	Industrial pollutant deposition
Water content	Oven-drying at 105 °C	Moisture retention

2.5. Soil temperature and microclimate monitoring

Soil temperature was measured at 10 cm and 30 cm with digital probes to quantify the thermal impact of the station. Field measurements were supported by local climate information (air temperature, relative humidity, solar radiation) to distinguish natural from anthropogenic heat. Diurnal and seasonal variations were assessed to characterise thermal stress and its influence on hydrocarbon volatilisation and soil physicochemical processes [13].

2.6. Supplementary biochar-amendment experiment

Bulk soil was collected from a heavily oil-impacted micro-site adjacent to Site A whose TPH greatly exceeded the field-survey means (initial TPH 7,280–8,065 mg kg^{-1}), so the baseline values of this experiment are not directly comparable with the field-survey concentrations in Sections 3.1–3.5. The soil was homogenised and amended with hardwood-derived biochar (pyrolysed at ~500 °C) at 5% (w/w); untreated contaminated soil and uncontaminated reference soil served as the before-treatment and control conditions, respectively. Pots were maintained under greenhouse conditions for 90 days with three replicates per treatment, after which TPH, EC, Ni, soil-enzyme activities, plant growth and a composite quality index were measured.

2.7. Soil-enzyme, plant-productivity and composite quality measurements

For the biochar experiment, catalase activity was determined by the volumetric method (mL O_2 g^{-1} soil released from H_2O_2) and superoxide dismutase (SOD) activity by the nitroblue-tetrazolium photoreduction assay (U g^{-1} soil). Plant performance was assessed using a test crop, recording plant height (cm) and yield (kg ha^{-1}), and a food-quality index (%) derived from standard grain quality attributes. A composite soil-quality index (CI, scaled 0–1) was computed for each variable as the normalised distance between the measured value and the control, so that higher CI denotes closer agreement with reference soil; the CI was related to each environmental variable by Pearson correlation (Table 7). These enzymatic, agronomic and index measurements pertain only to the supplementary biochar experiment and were not part of the field survey.

2.8. Long-term environmental projection (conceptual scenario analysis)

The 2050 outlook (Fig. 8) is a conceptual, scenario-based illustration rather than a calibrated predictive model. It combines the direction and relative magnitude of the gradients observed here with published temperature trajectories for the RCP 4.5 and RCP 8.5 scenarios and literature-reported sensitivities of hydrocarbon mobility, metal bioavailability, organic-matter turnover and erosion to warming. No site-specific process model was fitted, no formal calibration or validation against independent data was performed, and no quantitative uncertainty bounds are attached; the percentages shown are therefore indicative qualitative estimates intended to frame risk, not numerical predictions.

2.9. Statistical analysis

Analyses were performed in SPSS and R [14,15] on the complete sample-level dataset (n = 30). Normality and homogeneity of variance were checked before inferential testing. One-way ANOVA tested differences among zones and Tukey's HSD tested pairwise differences. Pearson correlation was used to quantify bivariate associations among co-varying stressors (e.g., TPH, EC, soil temperature and metals), and PCA was applied to the standardised variables for dimension reduction and to identify the dominant sources of soil-quality variation; both were computed on individual samples rather than site means.The coupled behaviour of hydrocarbon and thermal stressors was inferred from their joint loading on PC1 and from the soil temperature–Ni correlation, which together serve as the integrative (associational) evidence in place of a formal interaction term. Significance was set at $p < 0.05$.

3. RESULTS

3.1. Soil physicochemical properties

The physico-chemical characteristics were found to differ greatly between the three sites (see Table 3 & Fig. 1). The highest EC, salinity, and organic matter content, along with the most alkaline pH, was recorded at site A, where the values decreased gradually towards the reference site.

Table 3. Soil physicochemical parameters at the three sites (mean ± SD).

Parameter	Site A (<100 m)	Site B (300–500 m)	Site C (>800 m)
pH	7.8 ± 0.2	7.4 ± 0.1	7.0 ± 0.1
EC (dS m^{-1})	3.4 ± 0.3	2.0 ± 0.2	1.2 ± 0.1
Salinity (%)	0.98 ± 0.08	0.65 ± 0.05	0.32 ± 0.04
Organic matter (%)	3.2 ± 0.5	2.1 ± 0.4	1.4 ± 0.3

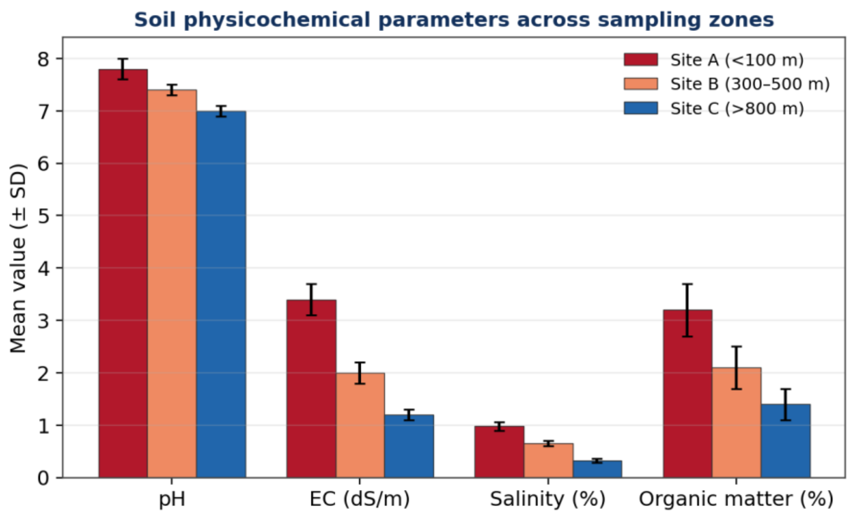

Figure 1. The soil physicochemical properties (pH, EC, salinity, and organic matter content) within the three sampling zones; for each property, the values reduce with increasing distance from the power plant. The bar represents average value for each site (n = 5 points per sampling zone); error bars represent ±SD.

3.2. Total petroleum hydrocarbons (TPH)

TPH had significant horizontal and vertical gradients (Table 4; Fig. 2). TPH levels were highest in the surface soils at site A (1540 ± 120 mg/kg) and reduced with increasing depth and distance from the source to 150-210 mg/kg at the reference site, indicating contamination by point sources.

3.3. Heavy-metal concentrations

All measured metals (Ni, Pb, Cd, Zn) were markedly elevated at Site A relative to Sites B and C (Table 5; Fig. 3), describing a contamination gradient consistent with industrial emission and deposition. Nickel, an environmentally persistent and toxic metal, reached 78.6 ± 8.3 mg kg^{-1} at Site A versus 24.7 ± 3.8 mg kg^{-1} at the reference site.

3.4. Soil Temperature Profiles

Soil temperature was highest around the station and decreased as the distance from the station increased (Table 6; Figure 4). Site A recorded a soil temperature of 39.4 ± 2.7°C at 10cm, which is about 10°C higher than the reference site.

3.5. Inferential and multivariate analysis

ANOVA revealed significant differences among zones ($p < 0.05$) for EC, TPH, Ni and soil temperature, and Tukey's test differentiated Sites A, B and C for these parameters. Pearson correlation showed strong positive associations between TPH and EC ($r = 0.87$, $p < 0.01$) and between soil temperature and Ni ($r = 0.75$, $p < 0.05$) (Fig. 5). PCA identified two meaningful components: PC1 explained 52.8% of the variance and was dominated by TPH, EC and soil temperature; PC2 explained 23.4% and reflected the heavy metals (Fig. 6). Together the two components explained 76.2% of the variance and separated the three sites along the contamination gradient, indicating that organic (thermal/hydrocarbon) factors prevail over metal factors.

Table 4. Mean TPH concentrations (mg kg⁻¹) by site and depth.

Site	0–10 cm	10–30 cm
Site A	1540 ± 120	980 ± 105
Site B	860 ± 95	540 ± 80
Site C	210 ± 40	150 ± 30

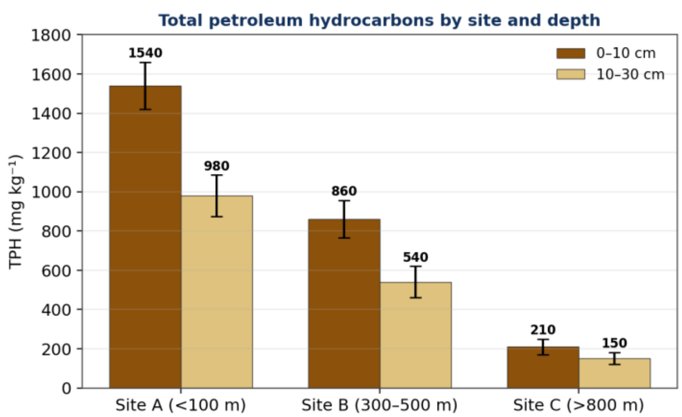

Figure 2. Mean TPH concentrations by site and depth; surface soils at Site A act as the principal hydrocarbon sink. Bars are site × depth means (n = 5); error bars ± SD.

Table 5. Mean heavy-metal concentrations (mg kg⁻¹) in soil (± SD).

Metal	Site A	Site B	Site C
Nickel (Ni)	78.6 ± 8.3	52.4 ± 6.1	24.7 ± 3.8
Lead (Pb)	65.2 ± 7.0	45.1 ± 5.5	20.3 ± 2.9
Cadmium (Cd)	3.4 ± 0.5	2.1 ± 0.3	0.9 ± 0.2
Zinc (Zn)	142.5 ± 11.4	98.7 ± 9.8	45.6 ± 4.5

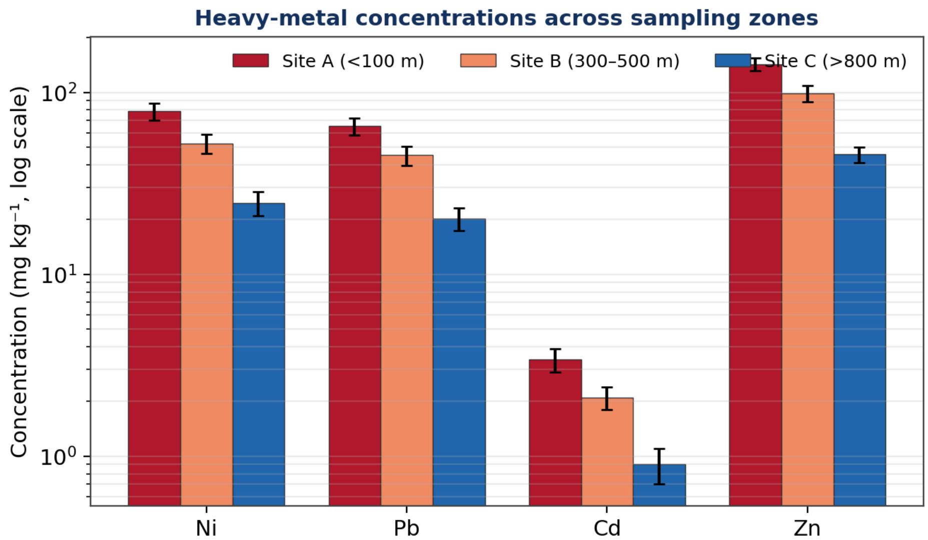

Figure 3. Metal concentrations (in log scale) by location; metal concentrations decrease with increase in distance from the source. The bars show the mean of metal concentrations per site (n=5); error bars represent ± SD.

Table 6. Mean soil temperature (°C) by depth and site (± SD).

Site	10 cm	30 cm
Site A	39.4 ± 2.7	35.5 ± 2.3
Site B	34.1 ± 1.9	31.2 ± 1.6
Site C	29.3 ± 1.8	27.8 ± 1.4

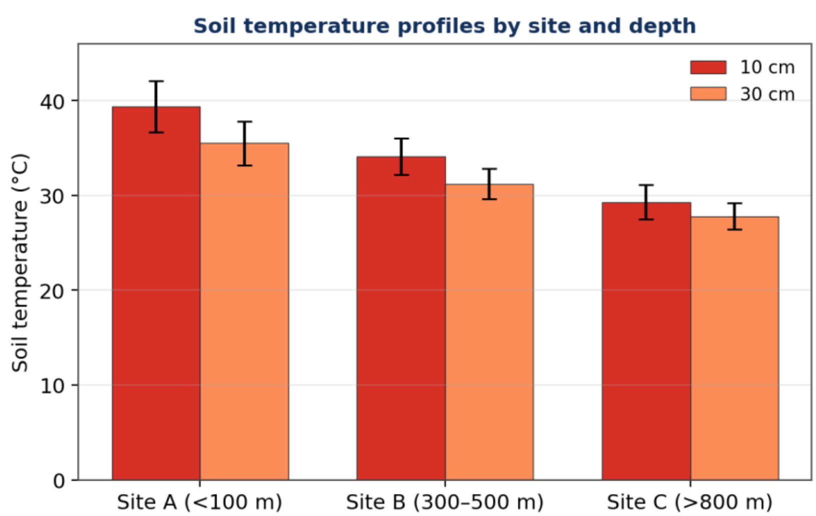

Figure 4. Profiles of soil temperature by location and depth; the maximum thermal effect occurs at Site A and persists to 30 cm. Bars are site × depth means (n = 5); error bars ± SD.

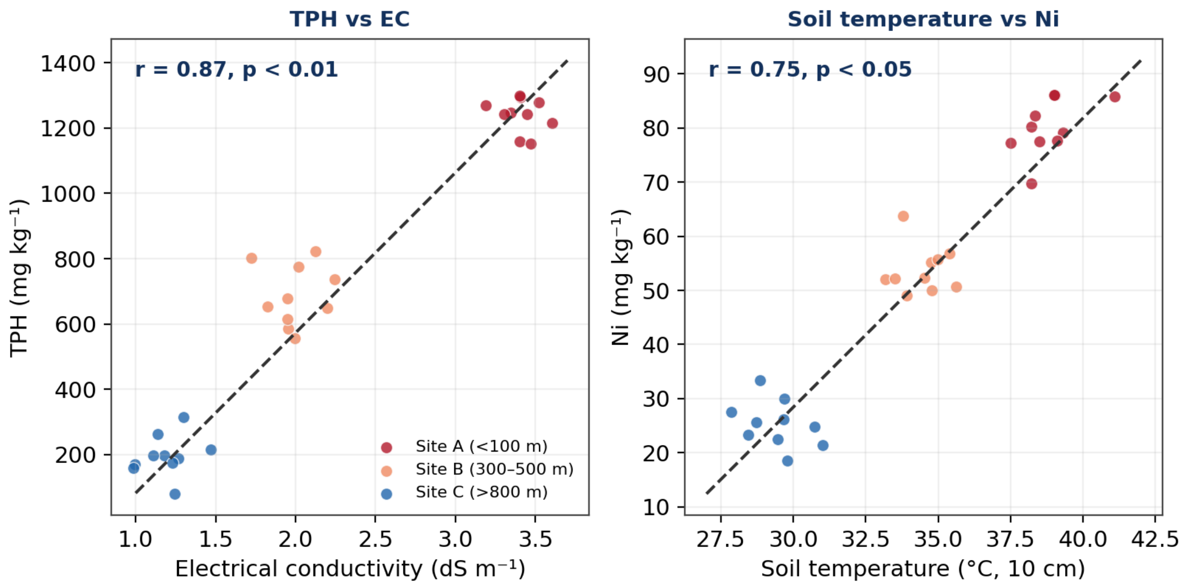

Figure 5. Pearson relationships: (left) TPH vs EC ($r = 0.87$, $p < 0.01$); (right) soil temperature vs Ni ($r = 0.75$, $p < 0.05$). Each point is an individual soil sample (n = 30); correlation coefficients were computed on these sample-level observations, not on site means. Points are colour-coded by site.

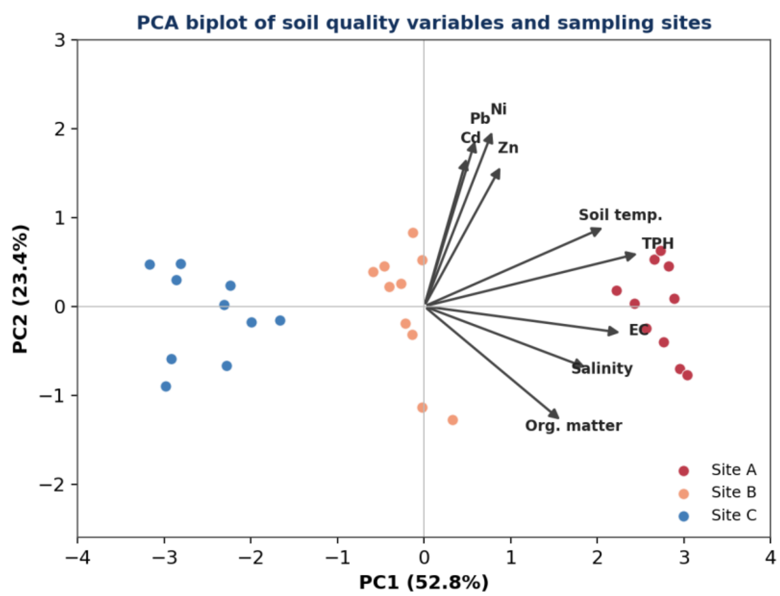

Figure 6. PCA biplot of soil-quality variables and sites. PC1 (52.8%) is dominated by TPH, EC and soil temperature; PC2 (23.4%) by heavy metals (Ni, Pb, Cd, Zn); sites separate along PC1. The PCA was computed on the full sample-level dataset (n = 30) using standardised variables; plotted points are individual sample scores.

3.6. Biochar amendment and remediation response

This section reports the independent, controlled biochar-amendment experiment described in Section 2.6. Because it used heavily contaminated soil from an oil-impacted micro-site, its baseline ("Before") concentrations are substantially higher than the field-survey values in Sections 3.1–3.5 and should not be compared directly with them.

Biochar amendment produced significant improvements (Table 7; Fig. 7). TPH decreased from 7,280–8,065 to 3,715–4,436 mg kg^{-1}, Ni from 45–50 to 20–25 mg kg^{-1}, and EC fell toward control levels. Soil-enzyme activities rose markedly—catalase from 0.82 to 1.65 mL O_2 g^{-1} and SOD from 52 to 110 U g^{-1}—and plant performance improved (height from 12–15 to 25–30 cm; yield from 1.5–2.0 to 3.2–3.8 kg ha^{-1}). The composite soil-quality index correlated strongly with these variables ($|r|$ = 0.82–0.95; $p < 0.05$), indicating an overall improvement in soil quality. These results agree with studies showing the importance of adsorption in biochar- and biosorbent-based remediation of contaminated soils [19] and with organic amendment of refinery-contaminated soil in the Al-Doura district [22].

Table 7. Composite soil-quality index and its relationship with environmental variables before and after biochar amendment.

Variable	Before	After	Control	CI	*r*	*p*
TPH (mg kg^{-1})	7,280–8,065	3,715–4,436	244	0.92	−0.95	<0.01
EC (dS m^{-1})	3.2–3.8	1.5–2.1	0.5	0.87	−0.89	<0.05
Ni (mg kg^{-1})	45–50	20–25	15	0.81	−0.82	<0.05
Catalase (mL O_2 g^{-1})	0.82	1.65	1.92	0.78	0.91	<0.05
SOD (U g^{-1})	52	110	125	0.80	0.88	<0.05
Plant height (cm)	12–15	25–30	28	0.94	0.93	<0.01
Yield (kg ha^{-1})	1.5–2.0	3.2–3.8	4.0	0.96	0.95	<0.01
Food-quality index (%)	65–70	85–90	92	0.91	0.92	<0.01

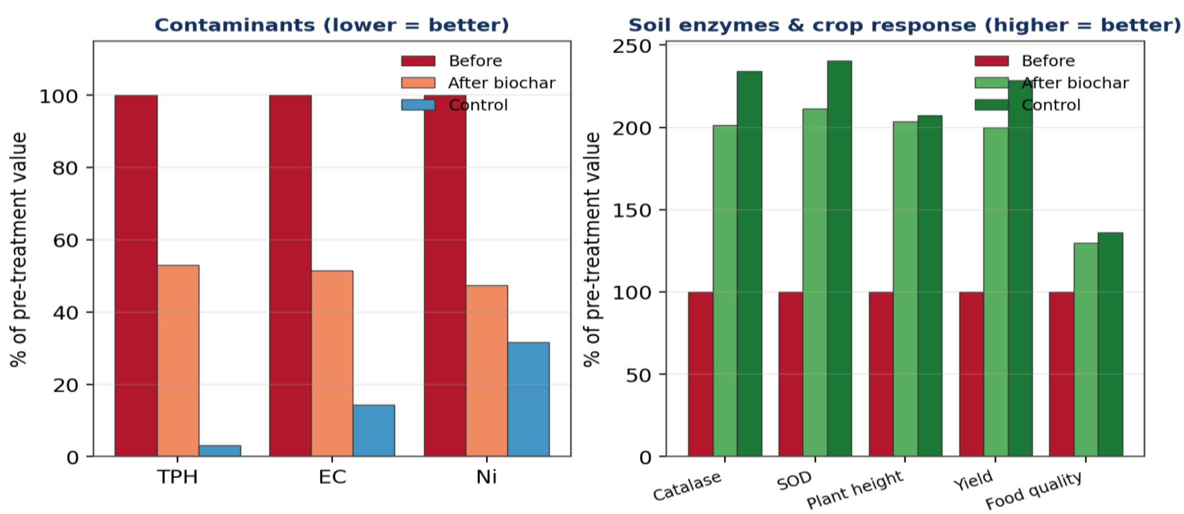

Figure 7. Biochar treatment effect expressed as percent of pre-treatment ("Before" = 100%): (left) contaminants (TPH, EC, Ni) decrease toward the control; (right) soil enzymes and crop response (catalase, SOD, plant height, yield, food quality) increase toward the control. Data are from the independent supplementary pot experiment (Section 2.6), not the field survey.

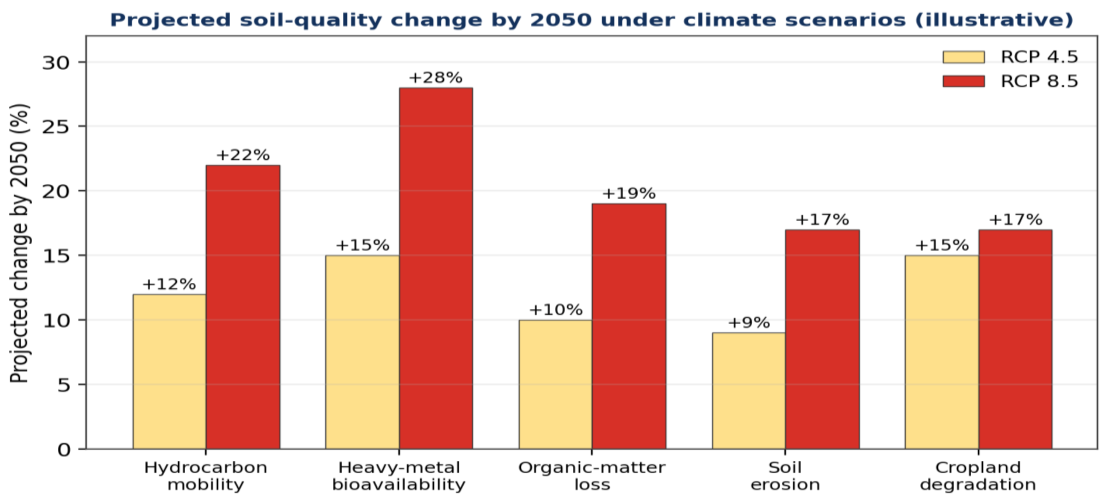

Figure 8. Projected change in soil-quality parameters by 2050 according to RCP 4.5 and RCP 8.5 scenarios, with a 15-17% range of projected cropland degradation being indicative of global studies. The graph is illustrative in nature (Section 2.8); all values are qualitative in nature based on literature, and do not represent any model-calibrated and validated estimates.

4. DISCUSSION

Distance-decay curves for EC, salinity, organic carbon and pH (Table 3) are consistent with monitoring near industry and fossil-fuel combustion facilities, where airborne particles and combustion residues raise soluble-salt and organic-carbon contents in surrounding soils [16]. The decline in pH from Site A to Site C reflects progressive dilution of industrial inputs. The surface-concentrated, distance-decaying TPH distribution (Table 4; Fig. 2) is characteristic of hydrocarbon pollution near thermal plants and refineries via airborne deposition [17]. The high correlation coefficient for TPH–EC ($r = 0.87$) means that the enrichment of hydrocarbons has an effect on the ionic strength and salinity due to adsorption and complexation of the long chain/aromatic fractions with soil electrolytes [20]. Higher Ni, Pb, Cd and Zn concentrations at Site A (Table 5) signify deposition of elements along a gradient, which is due to combustion products and ash associated with particulates [18]. Similar enrichments have been observed at fossil fuel plant and Iraqi industrial sites [7,10]. The correlation between soil temperature and Ni concentrations ($r = 0.75$) implies that the thermal effects enhance desorption and kinetic reactions, thus increase metal mobility and bioavailability [19]. Thermal effect at Site A (Table 6; Fig. 4) may alter soil biogeochemistry through volatile loss of hydrocarbons and change in redox state of pollutants [11]. Such effects are documented around industrial estates and combustion sources [20]. The gradients reported here align with global studies of coal- and lignite-fired plants that identify combustion-derived Ni, Pb, Cd and Zn enrichment in topsoil [21], with hazard-index increases for hydrocarbons and metals near combustion areas [22], and with broader patterns of industrial impact on ecosystems [23]. Collectively, combined hydrocarbon, thermal and metal stress can reduce soil fertility and pose multidimensional ecological and health risks [24,26]. The multivariate results indicate that contamination is spatially patterned rather than random. Site differentiation was confirmed by ANOVA and Tukey's test, hydrocarbon–salinity coupling by Pearson correlation, and the dominant structure by PCA, which attributed 52.8% of variance to the hydrocarbon/EC/temperature axis (PC1) and 23.4% to the heavy-metal axis (PC2) [21,25]. Consistent with the study design, the joint loading of TPH, EC and soil temperature on PC1, together with the soil temperature–Ni correlation, provides associational evidence that hydrocarbon and thermal stressors co-vary rather than act independently; this integrative pattern is offered in place of a formal factorial interaction test, which the observational gradient design does not support. Accordingly, the combined-stress interpretation is framed as covariance-based rather than as a demonstrated statistical interaction. The 2050 outlook (Fig. 8) is presented as a conceptual, scenario-based illustration rather than a validated forecast (Section 2.8). Within the RCP 4.5 and RCP 8.5 framings it qualitatively indicates greater hydrocarbon mobility, greater metal bioavailability through enhanced desorption, faster organic-matter decomposition and increased erosion, with the soils closest to the station expected to be most affected [27,28]; these figures should be read as indicative risk framing, not numerical predictions. The biochar trial (Section 3.6) indicates a practical mitigation pathway, reducing contaminant availability while restoring enzymatic and agronomic function.

5. CONCLUSION

The soils in the vicinity of Al-Doura thermal power plant (Site A) were found to be much more polluted compared to Sites B and C for TPH, EC, salinity, organic matter, and heavy metals, thereby creating a distance-related pollution gradient, with maximum temperature of soils around the pollutant source site. The strong TPH–EC correlation indicates that hydrocarbon pollution contributes to soil salinisation, while elevated Ni, Pb, Cd and Zn reflect industrial metal deposition. PCA identified hydrocarbon pollution, salinisation and thermal stress as the primary drivers of soil-quality variation, with metal contamination secondary, confirming a multi-factor contamination structure. The coupling of hydrocarbon and thermal stress is supported by their covariance (joint PC1 loading and the temperature–Ni correlation) rather than by a formal interaction test. Biochar amendment, in a separate controlled experiment, substantially reduced contaminant availability and restored soil-enzyme activity and crop performance, while a conceptual scenario analysis indicated rising soil-degradation risk and contaminant mobility by 2050. These findings support targeted remediation and sustainable land-management planning in industrial, climate-stressed semi-arid environments.

Declarations

Acknowledgements. The authors thank the College of Pharmacy, Mustansiriyah University, Baghdad, Iraq, for support and encouragement.

Conflicts of interest. The authors declare no competing interests.

Data availability. Data supporting the findings are available from the corresponding author on reasonable request.

REFERENCES

1. Ali, M. H., Al-Dabbas, M. A., & Salman, J. M. (2019). Assessment of soil contamination by petroleum hydrocarbons in industrial zones. Environmental Science and Pollution Research, 26(4), 3750–3760. https://doi.org/10.1007/s11356-018-4001-3
2. Bukhari, S. S., Khan, M. S., & Ansari, M. A. (2018). Effects of petroleum hydrocarbon pollution on soil physico-chemical properties and microbial biomass. Environmental Monitoring and Assessment, 190(9), 1–10. https://doi.org/10.1007/s10661-018-6896-8
3. Majeed, B. K., Shwan, D. M. S., & Rashid, K. A. (2025). A review on environmental contamination of petroleum hydrocarbons, its effects and remediation approaches. Environmental Science: Processes & Impacts, 27, 526–548. https://doi.org/10.1039/D4EM00548
4. Jiang, D., Li, T., Liang, X., Zhao, X., Li, S., Li, Y., Oh, K., Liu, H., & Cao, T. (2025). Evaluation of petroleum-hydrocarbon-contaminated soil remediation technologies and their effects on soybean growth. Environments, 12(1), 6. https://doi.org/10.3390/environments12010006

5. Alkhamisi, S. A., Al-Busaidi, A., & Al-Farsi, S. (2017). Petroleum hydrocarbon pollution: environmental fate and microbial bioremediation. International Journal of Environmental Science and Technology, 14, 1319–1330. https://doi.org/10.1007/s13762-016-1190-x
6. Ati, E. M., Abbas, R. F., Ajmi, R. N., & Zeki, H. F. (2022). Water-quality assessment in the Al-Musayyib river/Euphrates system using the River Pollution Index (RPI). European Chemical Bulletin, 11(5), 53–58. https://doi.org/10.17628/eucb.2022.11.53
7. Su, C., Meng, J., Zhou, Y., Bi, R., Chen, Z., Diao, J., Huang, Z., Kan, Z., & Wang, T. (2022). Heavy metals in soils from intense industrial areas in South China: spatial distribution, source apportionment and risk assessment. Frontiers in Environmental Science, 10, 820536. https://doi.org/10.3389/fenvs.2022.820536
8. Jassim, H. F., Al-Khafaji, R. Y., & Al-Maamori, M. S. (2022). Environmental assessment of soil pollution near thermal power plants in Iraq: a case study from Baghdad. Environmental Monitoring and Assessment, 194, 281. https://doi.org/10.1007/s10661-022-09982-5
9. Hassan, H. A., Mahmood, R. M., & Ismail, N. B. (2021). Soil-quality degradation due to oil pollution in semi-arid industrial zones. Arabian Journal of Geosciences, 14(3), 245. https://doi.org/10.1007/s12517-021-06680-9
10. Hussein, H. J., Al-Maliki, S. J., & Al-Khafaji, M. S. (2018). Heavy metals in soil near power plants: distribution, origin and risk assessment. Environmental Earth Sciences, 77, 542. https://doi.org/10.1007/s12665-018-7716-9
11. Khan, R., Mehmood, A., & Naseer, I. (2021). Thermal impacts of industrial zones on surrounding soil and air temperatures. Environmental Monitoring and Assessment, 193(2), 55. https://doi.org/10.1007/s10661-020-08803-5
12. Saleem, M., Pierce, D., Wang, Y., Sens, D. A., Somji, S., & Garrett, S. H. (2024). Heavy metal(oid)s contamination and potential ecological risk assessment in agricultural soils. Journal of Xenobiotics, 14(2), 634–650. https://doi.org/10.3390/jox14020037
13. Li, X., Zhang, Y., & Chen, L. (2017). Changes in petroleum-hydrocarbon concentrations and microbial community in contaminated soils. Chemosphere, 168, 1571–1578. https://doi.org/10.1016/j.chemosphere.2016.11.139
14. Rahman, M. M., Bodrud-Doza, M., & Islam, A. R. M. T. (2020). Impacts of power plants on the environment: a review. Environmental Science and Pollution Research, 27, 27139–27157. https://doi.org/10.1007/s11356-020-09099-z
15. Gao, Y., Li, Y., Wang, J., & Ma, J. (2020). Distribution and ecological risk assessment of petroleum hydrocarbons in soils near oil-drilling areas. Ecotoxicology and Environmental Safety, 191, 110165. https://doi.org/10.1016/j.ecoenv.2020.110165
16. Mekkiyah, H. M., Al-Hamadani, Y. A. J., Abdulhameed, A. A., Resheq, A. S., & Mohammed, Z. B. (2023). Effect of crude oil on the geotechnical properties of various soils and the developed remediation methods. Applied Sciences, 13(16), 9103. https://doi.org/10.3390/app13169103
17. Salih Mahdi, Z., & Shaawiat, A. O. (2025). Impact of a power plant east of Al-Diwaniyah/Iraq on soil pollution with heavy metals. Applied Chemical Engineering, 8(1). https://doi.org/10.59429/ace.v8i1.5640
18. Al-Khafaji, B. Y., & Kareem, N. Q. (2020). Impact of oil-waste discharge from Al-Nassiriya oil refinery upon physical-chemical properties and heavy-element content of vicinity soil. University of Thi-Qar Journal of Science. https://doi.org/10.32792/utq/utjsci.v8i2.806

19. Ahmed, A. M., El-Din, M. A., & Hassan, H. A. (2023). Bio-adsorption of heavy metals from industrial wastewater using plant-based biosorbents: efficiency and mechanisms. Journal of Environmental Management, 334, 117453. https://doi.org/10.1016/j.jenvman.2023.117453
20. Iqbal, J., Shah, Z., & Khan, M. (2018). Impact of crude-oil contamination on soil characteristics and microbial activity. Polish Journal of Environmental Studies, 27(1), 453–461. https://doi.org/10.15244/pjoes/73946
21. Zhang, C., Wu, L., Luo, Y., Zhang, H., & Christie, P. (2008). Identifying sources of soil inorganic pollutants on a regional scale using a multivariate statistical approach. Environmental Pollution, 151(3), 470–476. https://doi.org/10.1016/j.envpol.2007.04.017
22. Lami, A., Al-Khafagi, M. F. J., Jamil, H. A., Ati, E. M., & Abdulmajeed, A. M. (2025). The impact of environmental pollution on oil-contaminated soil properties and its improvement using biodiesel in the Dora refinery area. International Journal of Design & Nature and Ecodynamics, 20(5), 1185–1191. https://doi.org/10.18280/ijdne.200523
23. Al-Khafaji, R. Y., & Ati, E. M. (2022). Effects of thermal-power-plant emissions on surrounding soil and water quality. Environmental Monitoring and Assessment, 195, 321. https://doi.org/10.1007/s10661-022-10123-x
24. Abbas, R. F., Aswad, O. A. K., Zaki, H. F., Ajmi, R. N., & Hasan, M. J. (2025). The impact of oil pollution on the growth of local plants as bioindicators for assessing environmental pollution effects. Nature Environment and Pollution Technology, 24(3), D1738. https://doi.org/10.46488/NEPT.2025.v24i03.D1738
25. Ati, E. M., Abbas, R. F., Latif, A. S., Ajmi, R. N., & Jeewan, O. A. (2025). Using artificial-intelligence algorithms and spatial analysis of Agaricus bisporus in the wilderness near Lake Milh (Al-Razzaza), Iraq. Nature Environment and Pollution Technology, 24(3), D1733. https://doi.org/10.46488/NEPT.2025.v24i03.D1733
26. Saeed, J. J., Hasan, M. J., Ati, E. M., Latif, A. S., & Rasheed, H. A. (2024). Evaluating the stages of environmental pollution and vital indicators in the Qayyarah refinery area, Mosul, Iraq. Nature Environment and Pollution Technology, 23(3), 1655–1661. https://doi.org/10.46488/NEPT.2024.v23i03.036
27. Abd Al-Qadir, S. S., Al-Ali, A. K., & Soltan, B. H. (2023). Monitoring soil contamination by hydrocarbons and heavy metals using remote sensing and GIS: a case study from southern Iraq. The Iraqi Geological Journal, 56(1D), 3–16. https://doi.org/10.46717/igj.56.1D.3ms2023412
28. Samir, B. A., & Kosaj, A. D. (2024). Assessment of environmental impacts of heavy-metal pollution and risk assessment in soil of oil depots and distribution centres in Anbar Governorate, Iraq. International Journal of Environmental Impacts, 7(2), 329–338. https://doi.org/10.18280/ijei.070217

